Toll-Like Receptor Modulation of Murine Cerebral Malaria Is Dependent on the Genetic Background of the Host

Jason W. Griffith,[1] Christine O'Connor,[1] Ken Bernard,[1] Terrence Town,[2] Daniel R. Goldstein,[1] and Richard Bucala[1]

[1]Department of Internal Medicine and [2]Section of Immunobiology, Yale University, New Haven, Connecticut

Infection with *Plasmodium berghei* ANKA is a well-established model of human cerebral malaria (CM). We show herein that Toll-like receptor (TLR) signaling influences the development of lethal CM in *P. berghei* ANKA–infected mice. Modulation of outcome was dependent on genetic background, such that deletion of myeloid differentiation factor (MyD) 88 on the susceptible C57BL/6 background resulted in resistance to CM, whereas deletion of MyD88 on the resistant BALB/c background led to increased mortality. Our data show that MyD88 influenced the production of T helper–polarizing cytokines, including interferon (IFN)–γ, interleukin (IL)–4, and IL-17, as well as the total number of Foxp3$^+$ regulatory T (T_{reg}) cells in a manner dependent on host genetic background. In addition, mRNA levels of IFN-γ, CXCL10, and CXCL9 were strongly up-regulated in the brains of susceptible wild-type but not MyD88$^{-/-}$ infected mice. These results suggest that TLR signaling and host genetic background influences the pathogenesis of CM via modulation of cytokine production and T_{reg} cell numbers.

Plasmodium species, the causative agents of malaria, infect >300 million people annually, resulting in ~2.5 million deaths, mostly in children in sub-Saharan Africa [1–3]. Of those infected with the species *Plasmodium falciparum,* 1%–2% will develop cerebral malaria (CM), a complication that results in a significant proportion of malaria-associated mortality [4]. CM is a clinical entity with severe neurologic sequelae, including seizures, focal neurologic defects, and coma in patients with low to moderate parasitemia [5]. The pathologic hallmark of CM is sequestered parasitized red blood cells (pRBCs) and leukocytes in the brain microvasculature [6–8]. However, immune mechanisms also contribute to disease progression [6, 9–11]. Observations in human studies that elevated levels of serum proinflammatory cytokines correlate with CM support this hypothesis, but the exact immune effectors involved are still unclear from these observational and postmortem studies [12–15].

Germline-encoded innate immune system receptors for pathogen-associated molecular patterns (PAMPs) play an essential role in the host cytokine and adaptive immune response to infection [16–19]. PAMPs that have been identified in *Plasmodium* species include the glycosylphosphoinositol (GPI) posttranslational modification and hemozoin, which is produced during parasite heme metabolism. These moieties have been shown to activate the production of proinflammatory mediators by Toll-like receptor (TLR) 2/4 and TLR9, respectively [20, 21].

Recently, several studies have implicated TLR signaling in the control of malarial disease. Using a liver pathogenic strain of *Plasmodium berghei,* Adachi et al. demonstrated that myeloid differentiation factor (MyD) 88 was important in controlling the production of interleukin (IL)–12 and subsequent IL-12–dependent liver pathology [22]. Coban et al. demonstrated that TLR signaling is an important mediator of CM pathology in the *P. berghei* ANKA model in CM-susceptible C57BL/6 mice through modulation of cellular recruitment to the brain [23]. In the *P. berghei* ANKA model, the background genetics of the murine host are extremely im-

Received 16 February 2007; accepted 7 May 2007; electronically published 31 October 2007.

Potential conflicts of interest: none reported.

Financial support: National Institutes of Health (NIH; grants AI051306, AI042310 [to R.B.], and AIO164660 [to D.R.G.]); National Research Service Award/NIH/National Institute of Aging postdoctoral fellowship (to T.T.); NIH MSTP TG 5T32GM07205 (to J.W.G.).

Reprints or correspondence: Dr. Richard Bucala, Yale University, 300 Cedar St., TAC S525, PO Box 208031, New Haven, CT 06520-8031 (Richard.Bucala@Yale.edu).

The Journal of Infectious Diseases 2007; 196:1553–64

0022-1899/2007/19610-0019$15.00
DOI: 10.1086/522865

portant and modulate disease outcome. For instance, the Th1-biased C57BL/6 mouse is susceptible to the development of CM, whereas the Th2-biased BALB/c mouse is resistant [24]. How TLR signaling influences the pathogenesis of disease on these different genetic backgrounds is still unclear. In the present study, we investigated the role played by the TLR system in the pathogenesis of experimental CM in both the CM-susceptible C57BL/6 strain and the CM-resistant BALB/c strain.

MATERIALS AND METHODS

Mice. Wild-type (WT) C57BL/6 and BALB/c mice were purchased from the Jackson Laboratory. C57BL/6 MyD88$^{-/-}$, BALB/c MyD88$^{-/-}$, C57BL/6 TLR2$^{-/-}$, C57BL/6 TLR4$^{-/-}$, C57BL/6 TLR9$^{-/-}$, and C57BL/6 IL caspase enyzme–1 (ICE)$^{-/-}$ mice were used at 6–10 weeks of age, with sex, age, and background matched within experiments. All mice were backcrossed at least 7 times to their respective genetic background. Experiments were performed in compliance with the guidelines of the Yale University Institutional Animal Care and Use Committee.

P. berghei *ANKA infection.* All experiments used the *P. berghei* ANKA strain (MRA-311; Malaria Research and Reference Reagent Resource Center, American Type Culture Collection), which was maintained by periodic infection of C57BL/6 mice with frozen stocks of infected whole blood that was mixed 1:1 with glycerolyte (Baxter). For all experiments, mice were injected with 1×10^6 *P. berghei* ANKA pRBCs. Mice were monitored daily for neurologic signs of CM, including ataxia, paralysis, seizures, and coma. Parasitemia was assessed by counting pRBCs on smears of tail-vein blood samples stained with HEMA-3 (Fisher).

Serum and splenocyte cytokine production. On the indicated day after infection, serum was collected from mice by cardiac puncture, and their spleens were harvested. Spleens were disrupted and treated with 0.4 mg/mL liberase CI (Roche) for 30 min at 37°C. RBCs were lysed, and the remaining cells were plated at 5×10^6 cells/mL in 1 mL of RPMI 1640 plus L-glutamine (Gibco) with 10% fetal calf serum (FCS) and penicillin/streptomycin in 24-well plates for 72 h. Production of cytokines was quantified using the Beadlyte Mouse Multi-Cytokine Detection System 2 (Upstate), in accordance with the manufacturer's instructions, and was analyzed using the Bio-Rad Luminex platform.

Splenocyte CD3 stimulation. For CD3 stimulation experiments, 96-well plates were precoated with 10 μg/mL CD3 antibody (eBioscience) for 4 h at 37°C, and splenocytes from infected mice were plated at 1×10^6 cells/mL in 200 μL of RPMI 1640 plus L-glutamine supplemented with 10% FCS and penicillin/streptomycin for 72 h. Levels of interferon (IFN)–γ, IL-4, IL-10, and IL-17 were measured by ELISA (eBioscience).

Flow cytometry analysis. Isolated splenocytes from infected mice were RBC depleted and subjected to Foxp3 and CD4 staining by use of the anti–mouse Foxp3 staining set from eBiosciences, in accordance with the manufacturer's instructions. Anti-CD3ε (clone 145–2C11) from eBioscience was substituted for CD25. Flow cytometry was performed on a FACSCalibur instrument (BD) with CellQuest software and was analyzed with FlowJo software (version 8.5.2; Tree Star).

Reverse-transcriptase polymerase chain reaction (PCR). Total RNA was isolated from brains by use of Trizol (Invitrogen) and RNAeasy (Qiagen), in accordance with the manufacturer's instructions. RNA was reverse transcribed into cDNA by use of the ReactionReady First Strand cDNA Synthesis Kit (SuperArray), in accordance with the manufacturer's instructions. Primers for mouse IFN-γ, CXCL10, CXCL9, intercellular adhesion molecule (ICAM)–1, and GAPDH were purchased from SuperArray, and the reaction was run on the iCycler iQ (Bio-Rad), in accordance with the manufacturer's instructions. Gene expression was calculated using Chemidoc software (Bio-Rad) in relation to a standard curve of mouse universal RNA. Fold expression then was calculated using the ratio of the expressed gene of interest to that of GAPDH. The specificity of the PCR was confirmed by melt-curve analysis.

Histologic analysis. Tissues were sectioned and stained with hematoxylin-eosin according to standard practice and were visualized using a Nikon Microphot-FXA microscope at 40× magnification. Leukocyte adhesion was enumerated by morphologic analysis and reported as a percentage of vessels with leukoadhesion [25, 26]. Microhemorrhages were counted per brain slide and were identified by the presence of RBCs within the brain parenchyma, as described elsewhere [27].

Statistical analysis. Statistical analysis was preformed by Student's *t* test for all data except survival. Kaplan-Meier curves were generated for survival data, and significance was assessed by the log-rank test. $P < .05$ was considered to indicate significance.

RESULTS

Control of susceptibility to experimental CM by MyD88-dependent signaling on the basis of the genetic background of the host. To investigate the contribution of TLR signaling to CM, we inoculated *P. berghei* into mice bearing the genetic deletion of a key adaptor protein of TLR signaling, MyD88. We studied both the genetically susceptible (C57BL/6) and resistant (BALB/c) mouse strains and monitored them for neurologic defects and death, which occurred in susceptible strains between days 6 and 12 after infection. The mice that did not develop cerebral disease died of severe anemia after ~3 weeks, as has been reported previously [28]. As shown in figure 1*A* and 1*B*, 90% of WT mice on the susceptible C57BL/6 background developed neurologic signs and death consistent with CM, whereas <10% of mice deficient in MyD88 on this background developed CM ($P < .0001$). There was no difference in parasitemia

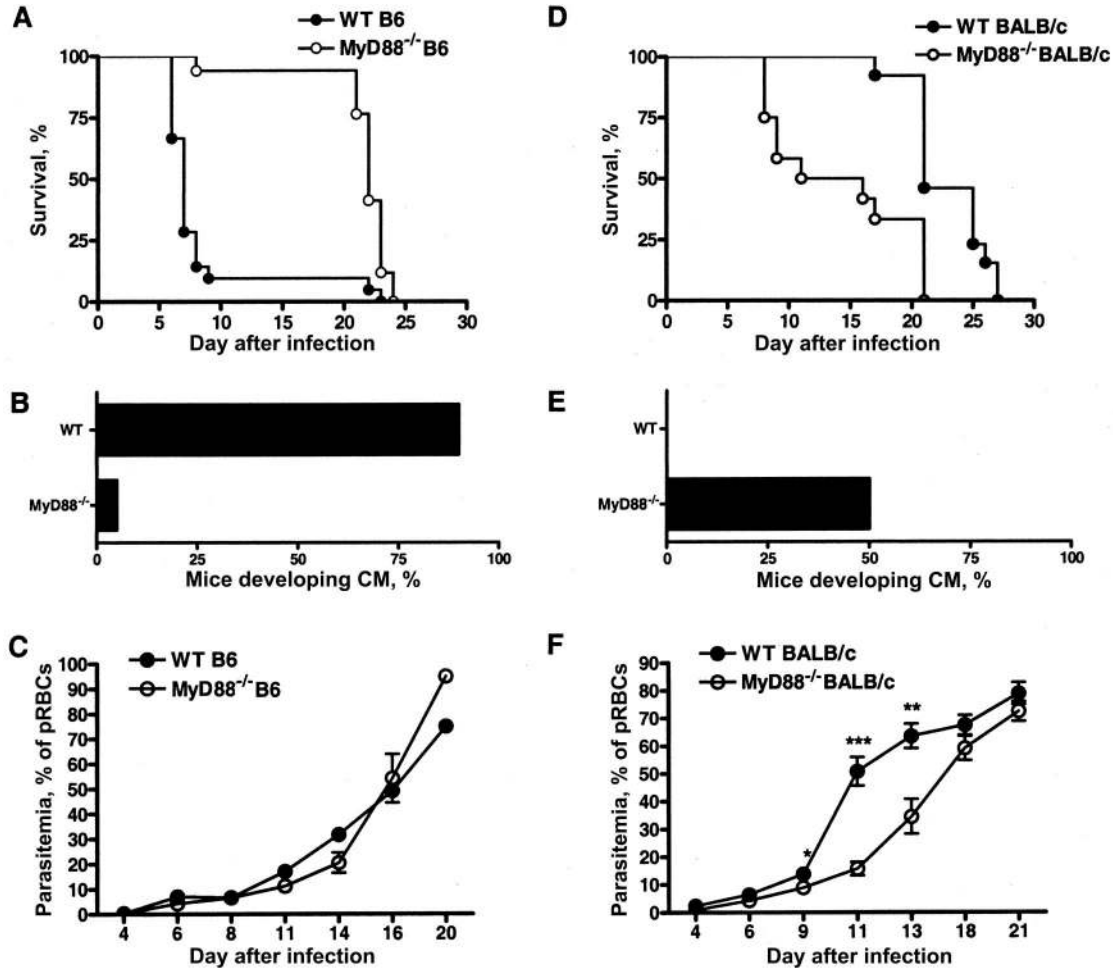

Figure 1. Influence of myeloid differentiation factor (MyD) 88 on susceptibility to cerebral malaria (CM). Wild-type (WT; *black circles*) and MyD88$^{-/-}$ *(white circles)* mice were infected with *Plasmodium berghei* ANKA. The percentage of survival, the development of CM, and parasitemia in MyD88$^{-/-}$ C57BL/6 ("B6" in the figure) (*A, B,* and *C*) and MyD88$^{-/-}$ BALB/c (*D, E,* and *F*) mice, compared with that in genetically matched WT control mice, were assessed. Survival (*A* and *D*) was monitored daily, and parasitemia (*C* and *F*) was measured every 2–3 days by thin blood smear. The percentage of mice developing CM (*B* and *E*) was calculated on the basis of the no. of mice presenting with CM symptoms or dying between days 6 and 12 after infection. For survival, $P < .0001$ for WT C57BL/6 ($n = 21$) vs. MyD88$^{-/-}$ C57BL/6 ($n = 17$) mice, and $P = .0003$ for WT BALB/c ($n = 13$) vs. MyD88$^{-/-}$ BALB/c ($n = 12$) mice. For parasitemia, $^{*}P < .05$, $^{**}P < .01$, and $^{***}P < .005$. Each infection is representative of 3 *(A)* or 4 *(B)* separate experiments. pRBC, parasitized red blood cells.

or hemoglobin levels between WT and MyD88$^{-/-}$ mice (figure 1*C* and data not shown).

In contrast to the susceptible C57BL/6 strain, WT BALB/c mice were completely resistant to CM and instead progressed to death from anemia and hyperparasitemia after 3–4 weeks. Surprisingly, MyD88$^{-/-}$ BALB/c mice demonstrated a significantly ($P = .0003$) increased susceptibility to death after infection with *P. berghei* (figure 1*D*). This increased susceptibility to death occurred between days 6–12 after infection at low levels of parasitemia and so was categorized as CM (figure 1*E*). Of note, this increase in death was correlated with a significant decrease in infected RBCs in MyD88$^{-/-}$ mice starting at day 9 after infection (figure 1*D*).

Development of CM reduced by TLR9 deficiency. MyD88 is an adaptor molecule that mediates signal transduction for TLR and the IL-1/IL-18 pathway, either of which could account for the protective effect of MyD88 deficiency on the C57BL/6 background. To study the role played by IL-1/IL-18 in the development of CM, we used mice deficient in ICE on the C57BL/6 background. ICE is required for the production of active IL-1β and IL-18 from their inactive proforms, and mice lacking this enzyme have deficient activation of this pathway [29]. As shown in figure 2*A*, ICE$^{-/-}$ mice did not show a significant difference in the development of lethal CM compared with WT mice (77% vs. 98%; $P \geq .05$), indicating that the IL-1/IL-18–dependent pathway is not necessary for the development of CM.

Ligands that may activate TLR signaling include the *Plasmodium*-encoded GPI anchor, which is recognized by TLR2 and TLR4 [20], and hemozoin, which is a metabolite of parasite hemoglobin digestion that is recognized by TLR9 [21]. To study

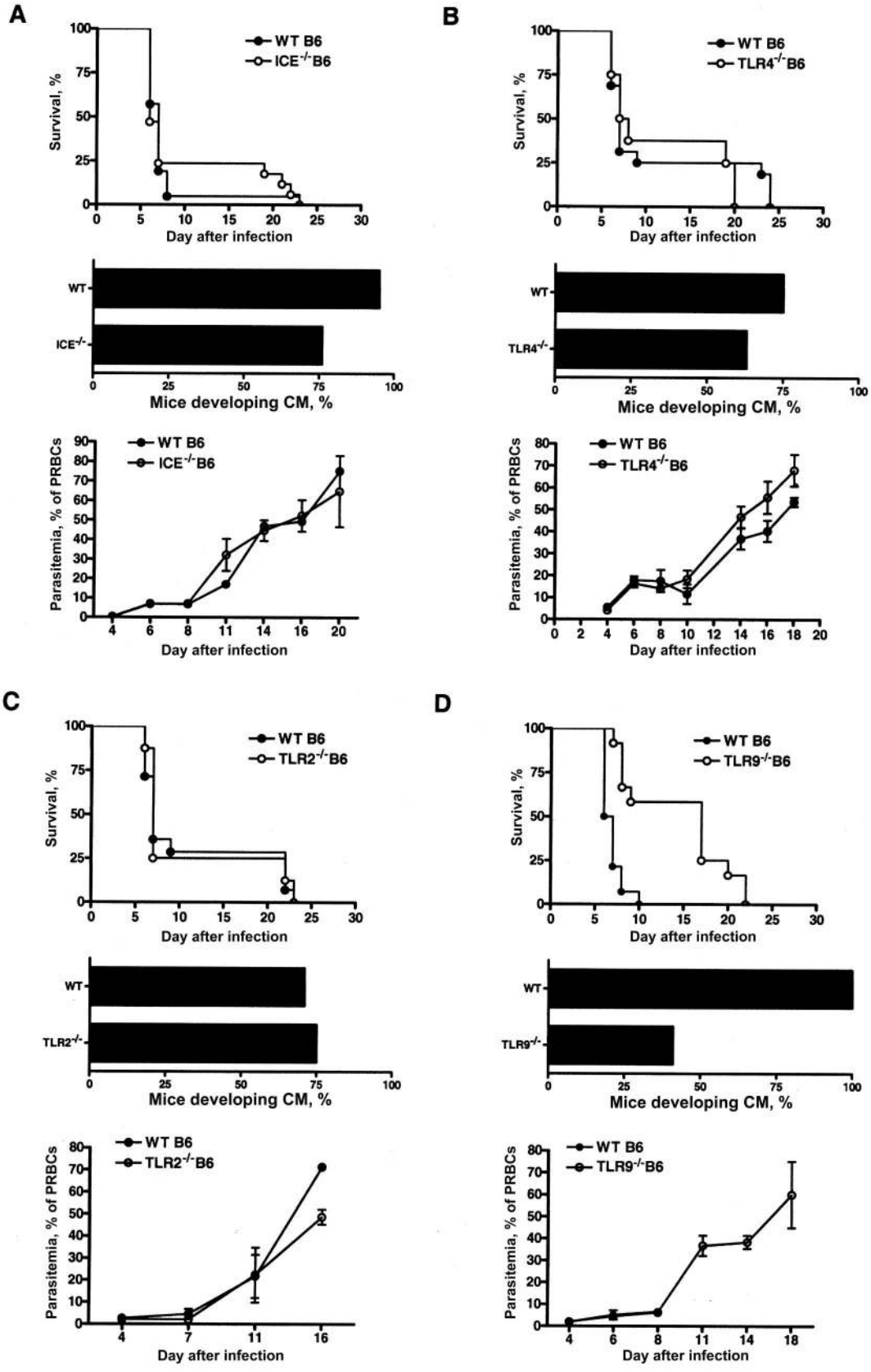

Figure 2. Control of the development of cerebral malaria (CM) by Toll-like receptor (TLR) 9. Wild-type (WT; *black circles*) or genetically deficient *(white circles)* mice were infected with *Plasmodium berghei* ANKA and assessed for survival and parasitemia. The percentage of survival, the development of CM, and parasitemia for WT C57BL/6 ("B6" in the figure) ($n = 21$) and interleukin caspase enyzme–1 $(ICE)^{-/-}$ C57BL/6 ($n = 17$) mice *(A),* WT C57BL/6 ($n = 16$) and $TLR4^{-/-}$ C57BL/6 ($n = 8$) mice *(B),* WT C57BL/6 ($n = 14$) and $TLR2^{-/-}$ C57BL/6 ($n = 8$) mice *(C),* and WT C57BL/6 ($n = 11$) and $TLR9^{-/-}$ C57BL/6 ($n = 12$) mice *(D)* were assessed by monitoring the mice daily and by obtaining blood smears every 2–3 days. Each infection is representative of 2 (*C* and *D*) or 3 (*A* and *B*) independent experiments. For survival of $TLR9^{-/-}$ mice *(B),* $P < .0001$.

the potential contribution of these TLRs to malaria, we inoculated C57BL/6 mice deficient in various TLRs with *P. berghei* ANKA. As demonstrated in figure 2*B,* mice deficient in TLR4 showed no significant difference in the development of lethal CM compared with WT mice (60% vs. 75%; $P \geq .05$). In addition, we did not detect a difference in the survival of mice with the genetic deletion of TLR2, as shown in figure 2*C* (71% vs. 75%; $P \geq .05$). In contrast, mice deficient in TLR9 had increased resistance to the development of lethal CM (41% [TLR9$^{-/-}$] vs. 100% [WT]; $P < .001$) (figure 2*D*). The degree of protection in TLR9$^{-/-}$ mice was not as complete as in C57BL/6 MyD88$^{-/-}$ mice, suggesting that other TLRs or components of MyD88-dependent signaling are important in the development of lethal CM.

Adhesion of leukocytes and microhemorrhage in brain vessels mediated by TLR signaling. CM mediated by *P. berghei* infection strongly correlates with adhesion of leukocytes in the brain microvasculature and microhemorrhages, whereby RBCs extravasate into the brain parenchyma [26, 30]. As shown in figure 3*A,* 3*B,* and 3*E,* WT C57BL/6 mice demonstrated a marked accumulation of mononuclear cells within 60% of brain vessels, compared with that in uninfected mice. MyD88$^{-/-}$ C57BL/6 mice had almost no detectable leukoadhesion (3%) (figure 3*C* and 3*E*). By contrast, TLR9$^{-/-}$ mice showed a lower number of adherent cells and fewer affected vessels (24.6%) than did WT mice but more than was observed in the MyD88$^{-/-}$ mice (figure 3*D* and 3*E*). In addition, TLR9$^{-/-}$ and MyD88$^{-/-}$ mice also had fewer microhemorrhages visible on histologic examination of brain sections than did WT mice (figure 3*F*).

Brains from both WT and MyD88$^{-/-}$ BALB/c mice demonstrated a very mild leukoadhesion that affected far fewer vessels than in C57BL/6 mice (figure 3*H* and 3*I*). However, brain sections from MyD88$^{-/-}$ BALB/c mice demonstrated a significant increase in the number of microhemorrhages per brain examined compared with brain sections from WT mice (figure 3*I* and 3*K*), suggesting that hemorrhage but not leukoadhesion may contribute to the increased mortality seen in *P. berghei*–infected MyD88$^{-/-}$ BALB/c mice (figure 1*D*).

Control of production of proinflammatory cytokines in vivo by MyD88. On the basis of the known function of MyD88 in the induction of innate cytokine expression [17, 18], we investigated the role played by MyD88 in the control of proinflammatory cytokine production by *P. berghei*–infected mice. In the case of WT C57BL/6 mice, we detected increased production of IFN-γ in serum (figure 4*A*) as well as increased production of tumor necrosis factor (TNF)–α (figure 4*C*) and IL-6 (figure 4*E*) by unstimulated splenocytes, which peaked on day 4 after infection. In comparison to WT mice, CM-resistant MyD88$^{-/-}$ C57BL/6 mice showed significantly reduced production of IFN-γ (figure 4*A*), TNF-α (figure 4*C*), and IL-6 (figure 4*E*). Both IFN-γ and TNF have been previously implicated in the development of CM [31, 32], and the present data support an important role for MyD88 in the control of the production of these systemic cytokines.

In comparison to the C57BL/6 strain, WT BALB/c mice produced less IFN-γ (figure 4*B*) on day 4 after infection but demonstrated comparable production of TNF-α (figure 4*D*) and IL-6 (figure 4*F*). However, in contrast to the observations in the C57BL/6 strain, MyD88$^{-/-}$ BALB/c mice demonstrated a small but significant increase in IFN-γ production on day 6 (figure 4*B*), compared with that in WT BALB/c mice. In addition, these MyD88$^{-/-}$ mice had a trend toward decreased production of TNF-α (figure 4*D*) and a significant decrease in the production of IL-6 (figure 4*F*), similar to what was seen in the C57BL/6 strain.

Control of the production of T cell–polarizing cytokines during malarial infection by the TLR pathway. In light of the effect of MyD88 deficiency on innate cytokine production in the CM model, we next investigated the secretion of the T helper–polarizing cytokines IFN-γ, IL-4, IL-10, and IL-17 by CD3-stimulated splenocytes isolated from *P. berghei*–infected mice on both the CM-susceptible (C57BL/6) and CM-resistant (BALB/c) genetic backgrounds. In splenocytes obtained from C57BL/6 mice, which is considered a Th1-permissive genetic background [24], IFN-γ (figure 5*A*), IL-4 (figure 5*C*), IL-10 (figure 5*E*), and IL-17 (figure 5*G*) were detected in supernatants, with peak levels at 4 days after infection. The production of these cytokines by C57BL/6 mice was reduced in mice lacking MyD88, with the largest decreases being for IFN-γ and IL-17.

When the same experiment was repeated in mice of the Th2-permissive BALB/c genetic background [33], the *P. berghei*–infected WT BALB/c mice were observed to produce significantly less IFN-γ than WT C57BL/6 mice (figure 5*A* and 5*B; P* = .0063). In addition, on the BALB/c background, MyD88 deficiency was associated with no change in IFN-γ production (figure 5*B; P* $\geq$ .05). Of note, CD3-stimulated splenocytes from infected MyD88$^{-/-}$ BALB/c mice had a >5-fold increase in the production of IL-4 (figure 5*D; P* < .0001). This large increase in IL-4 production was not accompanied by any effect of MyD88 on the production of IL-10 (figure 5*F*). As seen in the C57BL/6 stain, MyD88 deletion on the BALB/c background also led to a significant reduction in IL-17 production (figure 5*H*). Taken together, these data support a model whereby *P. berghei* infection in the setting of MyD88 deficiency promotes a selected change in cytokine production that is consistent with an enhanced Th2 response and that is further modified by the intrinsic Th1/Th2 genetic bias of the host strain.

Influence of MyD88 and genetic background on the percentage and total number of Foxp3$^+$ regulatory T (T_{reg}) cells. Recent data have suggested that a subset of T cells expressing CD4, CD25, and Foxp3 are T_{reg} cells that influence cytokine production and outcome in animal models of malaria [34–37] and in human malarial infection [38, 39]. Because TLR signaling is known to influence the activity of CD4$^+$CD25$^+$ T_{reg}

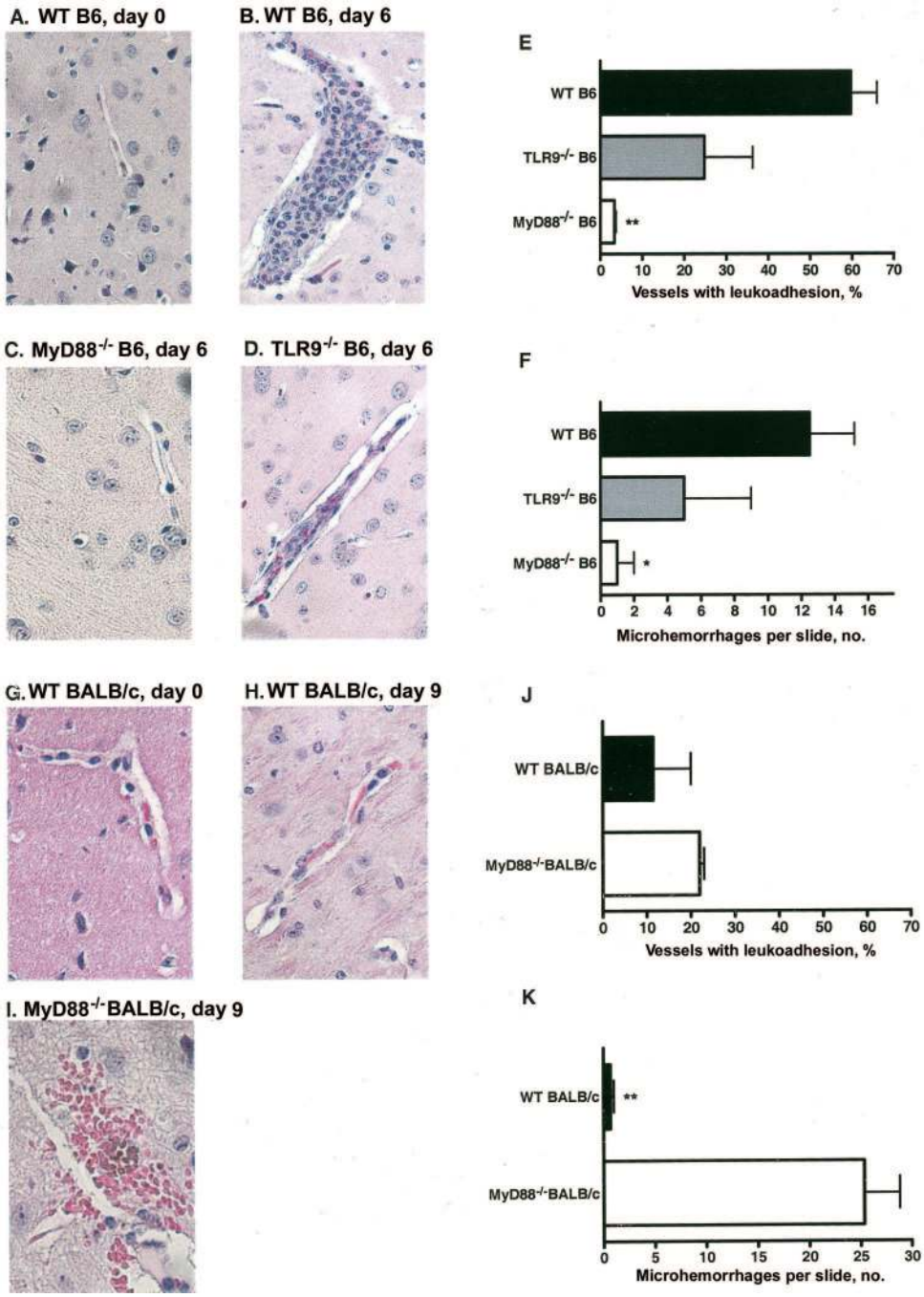

Figure 3. Mediation of adhesion of leukocytes to brain vessels in cerebral malaria (CM)–susceptible C57BL/6 mice by myeloid differentiation factor (MyD) 88 and Toll-like receptor (TLR) 9, and mediation of brain microhemorrhages in CM-resistant BALB/c mice by MyD88. Whole brains were isolated from uninfected WT C57BL/6 ("B6" in the figure) mice *(A),* day 6 *Plasmodium berghei*–infected WT C57LB/6 *(B),* MyD88$^{-/-}$ C57BL/6 *(C),* and TLR9$^{-/-}$ C57LB/6 *(D)* mice; uninfected WT BALB/c mice *(G);* and day 9 *P. berghei*–infected WT BALB/c *(H)* and MyD88$^{-/-}$ BALB/c *(I)* mice. Histological analysis was conducted after staining with hematoxylin-eosin. Representative data from 6–10 sections examined are shown. For WT C57BL/6 mice that developed CM, typical findings included lymphocytes within the brain vessels *(B)* and microhemorrhages, whereas MyD88$^{-/-}$ BALB/c mice demonstrated microhemorrhages *(I)* without significant leukoadhesion. Leukoadhesion was quantified by determining the percentage of vessels with adherent monocytes in the lumen in at least 4 fields per mouse with 4–10 mice per group (*E* and *J*); $P < .01$ for MyD88$^{-/-}$ vs. WT on the C57BL/6 background. Microhemorrhage was assessed by counting the no. of regions with red blood cells in tissue parenchyma of 4–8 brains per group (*F* and *K*); $P < .05$ for MyD88$^{-/-}$ vs. WT on the C57BL/6 background, and $P < .01$ for MyD88$^{-/-}$ vs. WT on the BALB/c background.

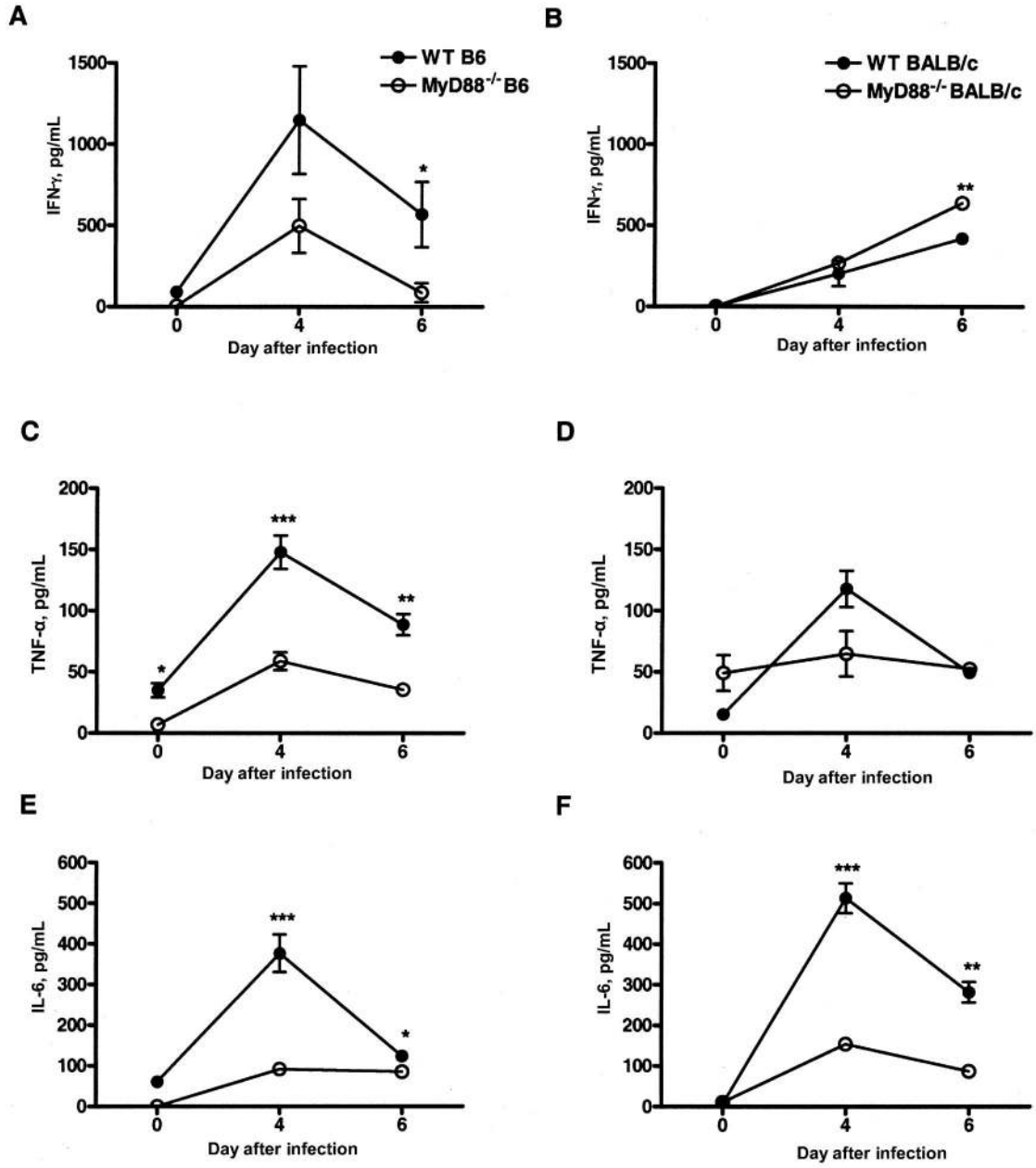

Figure 4. Control of proinflammatory cytokine production by myeloid differentiation factor (MyD) 88. In panels A and B, wild-type (WT; *black circles*) or MyD88$^{-/-}$ *(white circles)* C57BL/6 ("B6" in the figure) *(A)* or BALB/c *(B)* mice were infected with *Plasmodium berghei* ANKA, and, on the indicated day after infection, serum was harvested and analyzed for interferon (IFN)–γ production. In panels C–F, WT *(black circles)* or MyD88$^{-/-}$ *(white circles)* C57BL/6 (*C* and *E*) or BALB/c (*D* and *F*) mice were infected with *P. berghei* ANKA, and, on the indicated day after infection, their spleens were harvested and plated in vitro without addition of parasite antigen for 48 h. The culture supernatants were assayed for 12 cytokines by use of the Beadlyte Mouse Multi-Cytokine Detection System 2. Data shown for tumor necrosis factor (TNF)–α (*C* and *D*) and interleukin (IL)–6 (*E* and *F*) are mean values from 2 mice with spleens plated in triplicate. $^{*}P < .05$, $^{**}P < .01$, and $^{***}P < .005$ for WT vs. mutant mice. Each experiment was repeated twice.

cells [40], we examined the possibility that MyD88 influences the development of T_{reg} cells during *P. berghei* infection. For this analysis, we elected to monitor the percentage of CD4^{+}Foxp3^{+} T_{reg} cells and not CD4^{+}CD25^{+} T cells, because we noted a substantial proportion of CD4^{+}CD25^{+} T cells that were Foxp3 negative on day 6 of infection (data not shown). As can be seen in figure 6*A*, the percentage of CD4^{+}Foxp3^{+} T cells with respect to total CD3^{+} T cells decreased on day 6 of *P. berghei* infection in both WT and MyD88$^{-/-}$ C57BL/6 mice, but MyD88$^{-/-}$ mice had a significantly higher percentage of CD4^{+}Foxp3^{+} T cells than did WT mice on day 6 ($P < .05$). Despite the reduced percentages of these cells on day 6, we nevertheless found that the total numbers of CD4^{+}Foxp3^{+} T cells expanded in the WT and MyD88$^{-/-}$ C57BL/6 mouse strains (figure 6*B*). Consistent with a

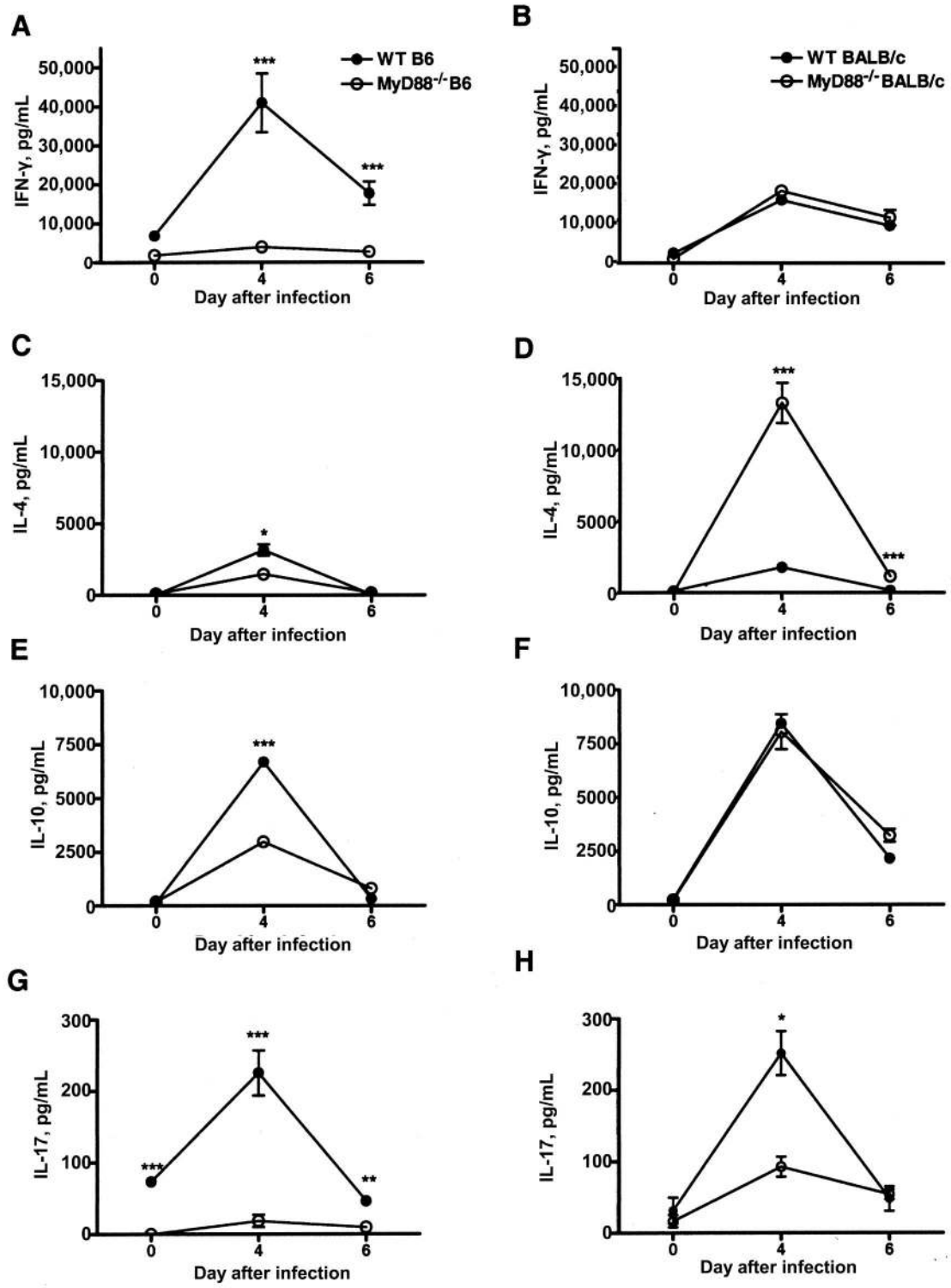

Figure 5. Control of production of T cell–polarizing cytokines by myeloid differentiation factor (MyD) 88. Wild-type (WT; *black circles*) or MyD88$^{-/-}$ *(white circles)* mice on either the C57BL/6 ("B6" in the figure) (*A, C, E,* and *G*) or BALB/c (*B, D, F,* and *H*) genetic background were infected with *Plasmodium berghei* ANKA, and, on the indicated day after infection, their spleens were harvested. Purified splenocytes were then stimulated with anti-CD3 for 72 h. Levels of interferon (IFN)–γ (*A* and *B*), interleukin (IL)–4 (*C* and *D*), IL-10 (*E* and *F*), and IL-17 (*G* and *H*) in the supernatant were measured by ELISA. Each point represents 2–4 mice, with triplicate plating. $^{*}P < .05$, $^{**}P < .01$, and $^{***}P < .005$ for WT vs. MyD88$^{-/-}$ mice. Each experiment is representative of at least 2 separate experiments.

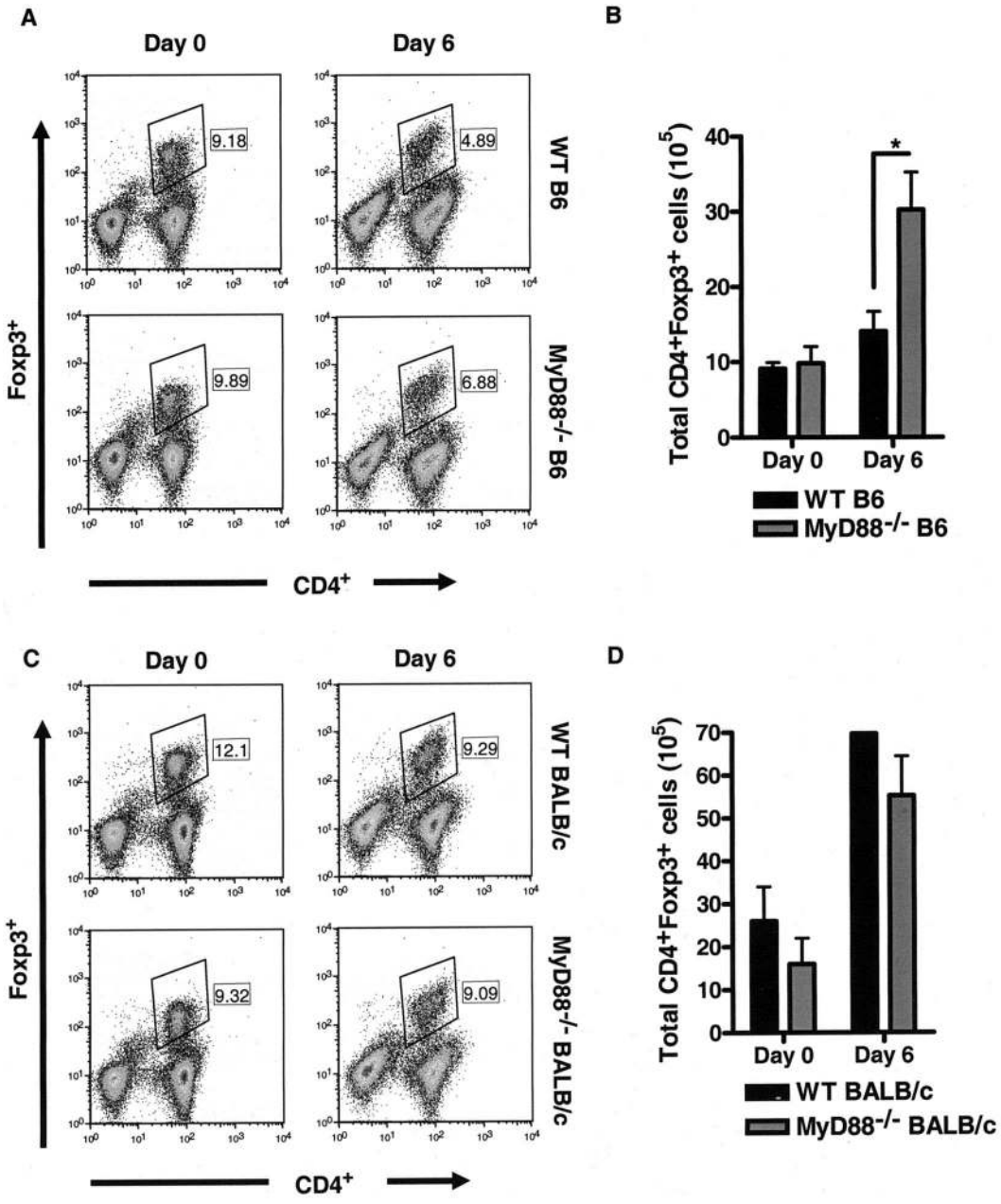

Figure 6. Influence of myeloid differentiation factor (MyD) 88 and genetic background on the expansion of Foxp3$^+$CD4$^+$ T cells during malarial infection. Splenocytes were harvested from wild-type (WT) and MyD88$^{-/-}$ C57BL/6 *(A)* or WT and MyD88$^{-/-}$ BALB/c *(C)* mice on day 0 or 6 after infection with *Plasmodium berghei* ANKA and were subjected to flow cytometry analysis for CD4 and Foxp3 expression after live cells were gated on CD3. The percentage of CD4$^+$Foxp3$^+$ cells (as shown in the representative plots of 3 experiments with 2–4 mice per group) decreased on day 6 for the C57BL/6 mice. Panels B and D show the total no. of CD4$^+$Foxp3$^+$ T cells for WT C57BL/6 *(black bars)* or MyD88$^{-/-}$ C57BL/6 *(gray bars) (B)* or WT BALB/c *(black bars)* and MyD88$^{-/-}$ BALB/c *(gray bars) (D)* mice on day 0 or 6 after infection. A significant difference between WT C57BL/6 and MyD88$^{-/-}$ C57BL/6 was noted on day 6 (*$P < .05$, Student's *t* test).

role for TLR signaling in modulating the activity of T_{reg} cells, we found that MyD88$^{-/-}$ C57BL/6 mice had a significantly increased number of CD4$^+$Foxp3$^+$ T cells, compared with that in WT mice, on day 6.

When WT and MyD88$^{-/-}$ BALB/c mice were analyzed in the same fashion (figure 6*C*), we noted increased percentages of CD4$^+$Foxp3$^+$ T cells on both days 0 and 6, compared with those in C57BL/6 mice, and noted that the percentage of CD4$^+$Foxp3$^+$ T cells did not decrease significantly on day 6 of infection. Similarly, when the total numbers of CD4$^+$Foxp3$^+$ T cells were analyzed (figure 6*D*), the numbers for both WT and MyD88$^{-/-}$ BALB/c mice were ~2-fold higher than that for C57BL/6 mice on both days 0 and 6 and more than doubled from day 0 to day 6. We did not note any significant difference in cell numbers be-

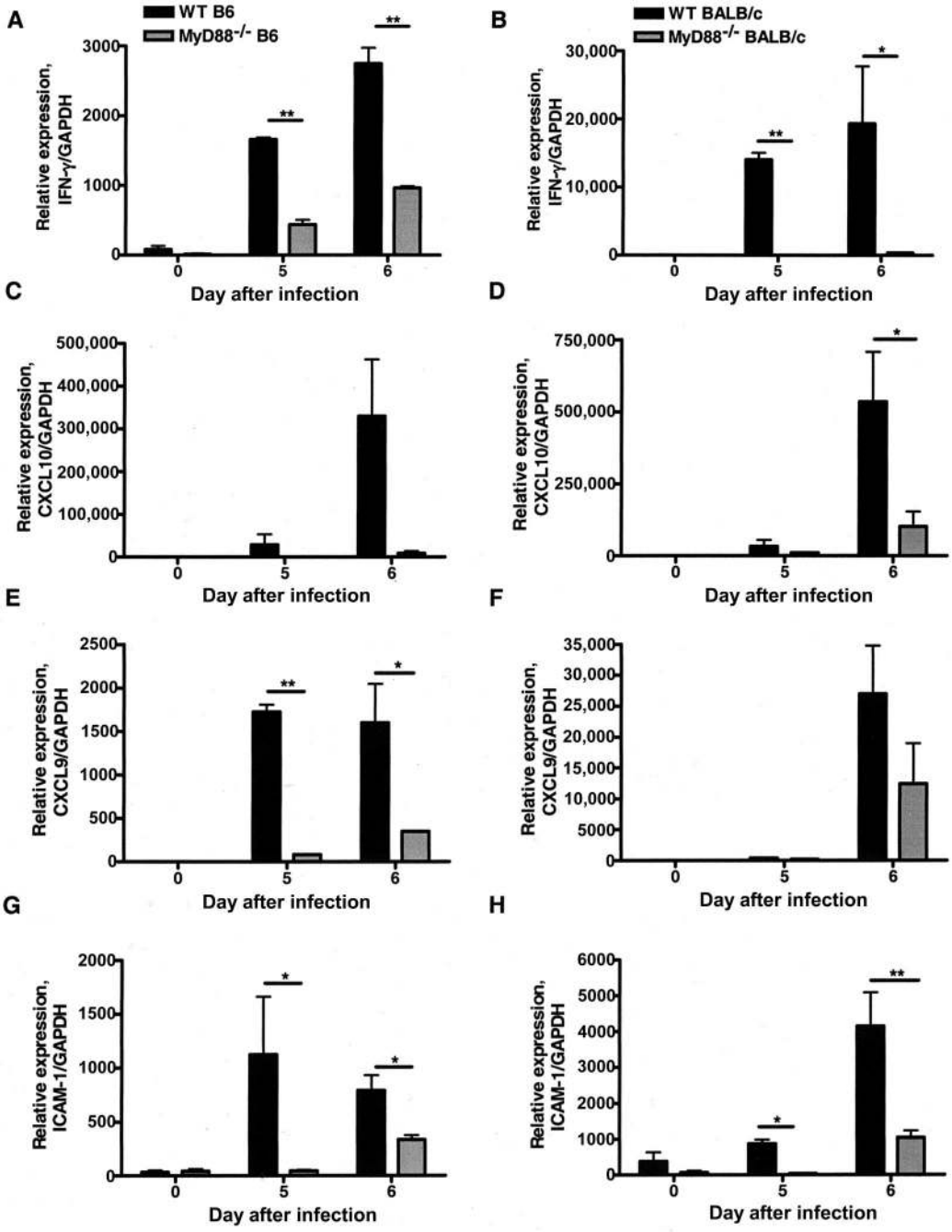

Figure 7. Induction of myeloid differentiation factor (MyD) 88–dependent mRNA expression of brain cytokine, chemokine, and adhesive molecules by *Plasmodium berghei* ANKA infection. Whole brains were isolated from wild-type (WT; *black bars*) or MyD88$^{-/-}$ *(gray bars)* C57BL/6 ("B6" in the figure) (*A, C, E,* and *G*) or BALB/c (*B, D, F,* and *H*) mice infected with *P. berghei* ANKA for the indicated no. of days. Tissue mRNA expression of interferon (IFN)–γ (*A* and *B*), CXCL10 (*C* and *D*), CXCL9 (*E* and *F*), and intercellular adhesion molecule (ICAM)–1 (*G* and *H*) was analyzed by real-time reverse-transcriptase polymerase chain reaction and presented as relative units normalized to the GAPDH control (mean ± SD) for 2–3 mice from each group. $^{*}P < .05$ and $^{**}P < .01$. The figure is representative of 1 of 2 separate experiments.

tween WT and MyD88$^{-/-}$ mice on either day. These data suggest the genetic background of the host influences the number of T_{reg} cells during infection, such that the resistant BALB/c strain has ~2-fold more T_{reg} cells at all times tested. Furthermore, the influence of MyD88 during infection of C57BL/6 mice suggests that TLR signaling may play an important role in modulating T_{reg} cell number. The association between decreased T_{reg} cell percentage and pathogenesis also suggests that these cells may influence the outcome of CM disease.

Regulation of the production of chemokines and adhesion molecules in the brains of* P. berghei*–infected mice by MyD88. Given the significant role played by MyD88 in regulating sys-

temic IFN-γ production, we analyzed the local IFN-γ response in the brains of *P. berghei*–infected mice. Figure 7*A* and 7*B* demonstrates that brain tissue from *P. berghei*–infected C57BL/6 and BALB/c mice, respectively, has prominent IFN-γ mRNA expression on days 5 and 6, which corresponds to the period immediately before the onset of CM lethality (figure 1*A*). Local tissue expression of IFN-γ was significantly lower in MyD88$^{-/-}$ mice than in WT control mice. Because IFN-γ is known to up-regulate the expression of a subset of CXC chemokines, including CXCL10 and CXCL9 [41], we hypothesized that these chemokines could play a role in the recruitment of leukocytes to the brain. As demonstrated in figure 7*C–F,* the mRNA for these chemokines was strongly and significantly up-regulated in either WT C57BL/6 or BALB/c mice, compared with that in MyD88$^{-/-}$ C57BL/6 or BALB/c mice. As shown in figure 7*G* and 7*H,* expression of the adhesion molecule ICAM-1 was also up-regulated in WT mice, but not in MyD88$^{-/-}$ mice, on days 5 and 6 after infection in both C57BL/7 and BALB/c strains. The expression of IFN-γ, CXCL10, CXCL9, and ICAM-1 was considerably higher than that of C57BL/6 in BALB/c strains.

DISCUSSION

The present study provides support for a role for TLR-dependent cytokine responses in the pathogenesis of experimentally induced CM. C57LB/6 mice deficient in MyD88 are protected from lethal CM. By contrast, on the CM-resistant BALB/c background, MyD88 deficiency was associated with early death despite a reduction in parasitemia during the midphase of the infection. These MyD88$^{-/-}$ BALB/c mice demonstrated increased microhemorrhages in the brain, which may mediate death.

Previous studies have suggested that early production of the Th1 cytokines IFN-γ and TNF-α contribute to the pathogenesis of CM [42]. In accord with the findings of these studies, we observed an effect of MyD88 on the selective production of Th1, Th2, and IL-17 cytokines that varied with the genetic background of the host and correlated with survival. On the CM-susceptible Th1-permissive C57BL/6 background, MyD88 deletion was associated with a reduction in IFN-γ and TNF-α production. However, on the CM-resistant Th2-permissive BALB/c background, MyD88 deletion led to a very large increase in the production of the Th2 cytokine IL-4, with limited effect on the production of IFN-γ. How this robust IL-4 response contributes to the pathogenesis of CM remains unclear. Thus, TLR signaling through MyD88 skews the production of polarizing cytokines toward a Th1 profile. This bias is pathogenic in a mouse strain that responds with a strong Th1 response to malarial infection (C57BL/6) but is protective in strains that primarily respond with a Th2 response (BALB/c).

One possible mechanism for the noted difference in cytokine secretion may be the differential expansion of CD4$^+$Foxp3$^+$ T_{reg} cells. Studies using the *P. berghei* and *Plasmodium yoelii* strains in mice have demonstrated that the population of Foxp3$^+$ T_{reg} cells expand and modulate cytokine production during acute infection [34–37]. How these cells modulate the course of infection and pathology is still unclear, given the rapid regeneration of Foxp3$^+$ T_{reg} cells after depletion with anti-CD25 and concerns that the anti-CD25 antibody also depletes activated T cells [43]. In the present study, we have noted that the protected BALB/c mice have a significantly higher expansion of Foxp3$^+$ T_{reg} cells than do C57BL/6 mice during infection. Furthermore, although Foxp3$^+$ T_{reg} cells expand in WT C57BL/6 mice, the total proportion of these cells to the total T cell number decreases, compared with that in BALB/c mice. MyD88$^{-/-}$ C57BL/6 mice have a significantly increased proportion and total expansion of Foxp3$^+$ T_{reg} cell numbers compared with WT C57BL/6 mice, which implies that TLR signaling may control the expansion of T_{reg} cells on this background.

Locally, in the brains of infected mice, we observed an early and significant MyD88-dependent increase in the mRNA levels of the IFN-γ–inducible chemokines CXCL10 and CXCL9. These observations suggest that CXCL10 and CXCL9 and their receptor CXCR3 may play an important pathogenic role in the development of CM and may contribute to the recruitment of leukocytes to the brain vasculature. It remains unclear why WT BALB/c mice have significantly higher mRNA levels of these chemokines than do C57BL/6 mice without evidence of increased leukocyte recruitment.

In summary, the pathologic outcome of *P. berghei* infection is dependent on the host expression of T cell–polarizing cytokines and Foxp3$^+$ T_{reg} cells, which is influenced by TLR signaling through MyD88 and the genetic background of the host. These data suggest that CM in humans may be a diverse disease that is either Th1 biased and associated with leukoadhesion or Th2 biased and associated with hemorrhage—a finding that may explain some of the different pathologies seen in human autopsy studies of CM [8]. Furthermore, these findings support the possibility that clinical expression of CM also may vary in the setting of helminthic coinfections, which are common in malarial areas and are associated with Th2 cytokine responses.

Acknowledgments

We thank Ruslan Medzhitov and Richard Flavell for providing the knockout mice used in these studies and Thomas McCutchan for providing *Plasmodium berghei* parasites to the Malaria Research and Reference Reagent Resource Center.

References

1. Snow RW, Guerra CA, Noor AM, Myint HY, Hay SI. The global distribution of clinical episodes of *Plasmodium falciparum* malaria. Nature **2005**; 434:214–7.
2. Guerra CA, Snow RW, Hay SI. Mapping the global extent of malaria in 2005. Trends Parasitol **2006**; 22:353–8.
3. Breman JG. The ears of the hippopotamus: manifestations, determinants, and estimates of the malaria burden. Am J Trop Med Hyg **2001**; 64:1–11.

4. Rowe AK, Rowe SY, Snow RW, et al. The burden of malaria mortality among African children in the year 2000. Int J Epidemiol **2006**; 35:691–704.
5. Olumese PE, Gbadegesin RA, Adeyemo AA, Brown B, Walker A. Neurological features of cerebral malaria in Nigerian children. Ann Trop Paediatr **1999**; 19:321–5.
6. Miller LH, Baruch DI, Marsh K, Doumbo OK. The pathogenic basis of malaria. Nature **2002**; 415:673–9.
7. Brown H, Hien TT, Day N, et al. Evidence of blood-brain barrier dysfunction in human cerebral malaria. Neuropathol Appl Neurobiol **1999**; 25:331–40.
8. Silamut K, Phu NH, Whitty C, et al. A quantitative analysis of the microvascular sequestration of malaria parasites in the human brain. Am J Pathol **1999**; 155:395–410.
9. Hunt NH, Golenser J, Chan-Ling T, et al. Immunopathogenesis of cerebral malaria. Int J Parasitol **2006**; 36:569–82.
10. Schofield L, Grau GE. Immunological processes in malaria pathogenesis. Nat Rev Immunol **2005**; 5:722–35.
11. Coltel N, Combes V, Hunt NH, Grau GE. Cerebral malaria—a neurovascular pathology with many riddles still to be solved. Curr Neurovasc Res **2004**; 1:91–110.
12. Day NP, Hien TT, Schollaardt T, et al. The prognostic and pathophysiologic role of pro- and antiinflammatory cytokines in severe malaria. J Infect Dis **1999**; 180:1288–97.
13. Grau GE, Taylor TE, Molyneux ME, et al. Tumor necrosis factor and disease severity in children with falciparum malaria. N Engl J Med **1989**; 320:1586–91.
14. Kwiatkowski D, Hill AV, Sambou I, et al. TNF concentration in fatal cerebral, non-fatal cerebral, and uncomplicated *Plasmodium falciparum* malaria. Lancet **1990**; 336:1201–4.
15. Brown H, Turner G, Rogerson S, et al. Cytokine expression in the brain in human cerebral malaria. J Infect Dis **1999**; 180:1742–6.
16. Iwasaki A, Medzhitov R. Toll-like receptor control of the adaptive immune responses. Nat Immunol **2004**; 5:987–95.
17. Pasare C, Medzhitov R. Toll-like receptors: linking innate and adaptive immunity. Adv Exp Med Biol **2005**; 560:11–8.
18. Akira S, Takeda K, Kaisho T. Toll-like receptors: critical proteins linking innate and acquired immunity. Nat Immunol **2001**; 2:675–80.
19. Takeda K, Akira S. Roles of Toll-like receptors in innate immune responses. Genes Cells **2001**; 6:733–42.
20. Krishnegowda G, Hajjar AM, Zhu J, et al. Induction of proinflammatory responses in macrophages by the glycosylphosphatidylinositols of *Plasmodium falciparum:* cell signaling receptors, glycosylphosphatidylinositol (GPI) structural requirement, and regulation of GPI activity. J Biol Chem **2005**; 280:8606–16.
21. Coban C, Ishii KJ, Kawai T, et al. Toll-like receptor 9 mediates innate immune activation by the malaria pigment hemozoin. J Exp Med **2005**; 201:19–25.
22. Adachi K, Tsutsui H, Kashiwamura S, et al. *Plasmodium berghei* infection in mice induces liver injury by an IL-12- and toll-like receptor/myeloid differentiation factor 88-dependent mechanism. J Immunol **2001**; 167:5928–34.
23. Coban C, Ishii KJ, Uematsu S, et al. Pathological role of Toll-like receptor signaling in cerebral malaria. Int Immunol **2007**; 19:67–79.
24. de Kossodo S, Grau GE. Profiles of cytokine production in relation with susceptibility to cerebral malaria. J Immunol **1993**; 151:4811–20.
25. Lou J, Lucas R, Grau GE. Pathogenesis of cerebral malaria: recent experimental data and possible applications for humans. Clin Microbiol Rev **2001**; 14:810–20.
26. Hearn J, Rayment N, Landon DN, Katz DR, De Souza JB. Immunopathology of cerebral malaria: morphological evidence of parasite sequestration in murine brain microvasculature. Infect Immun **2000**; 68:5364–76.
27. Sanni LA, Jarra W, Li C, Langhorne J. Cerebral edema and cerebral hemorrhages in interleukin-10-deficient mice infected with *Plasmodium chabaudi*. Infect Immun **2004**; 72:3054–8.
28. Grau GE, Fajardo LF, Piguet PF, Allet B, Lambert PH, Vassalli P. Tumor necrosis factor (cachectin) as an essential mediator in murine cerebral malaria. Science **1987**; 237:1210–2.
29. Fantuzzi G, Dinarello CA. Interleukin-18 and interleukin-1 beta: two cytokine substrates for ICE (caspase-1). J Clin Immunol **1999**; 19:1–11.
30. Engwerda CR, Mynott TL, Sawhney S, De Souza JB, Bickle QD, Kaye PM. Locally up-regulated lymphotoxin alpha, not systemic tumor necrosis factor alpha, is the principle mediator of murine cerebral malaria. J Exp Med **2002**; 195:1371–7.
31. Grau GE, Heremans H, Piguet PF, et al. Monoclonal antibody against interferon gamma can prevent experimental cerebral malaria and its associated overproduction of tumor necrosis factor. Proc Natl Acad Sci USA **1989**; 86:5572–4.
32. Lucas R, Juillard P, Decoster E, et al. Crucial role of tumor necrosis factor (TNF) receptor 2 and membrane-bound TNF in experimental cerebral malaria. Eur J Immunol **1997**; 27:1719–25.
33. Taylor-Robinson AW, Phillips RS, Severn A, Moncada S, Liew FY. The role of TH1 and TH2 cells in a rodent malaria infection. Science **1993**; 260:1931–4.
34. Hisaeda H, Maekawa Y, Iwakawa D, et al. Escape of malaria parasites from host immunity requires CD4+ CD25+ regulatory T cells. Nat Med **2004**; 10:29–30.
35. Wu Y, Wang QH, Zheng L, et al. *Plasmodium yoelii:* distinct $CD4^+CD25^+$ regulatory T cell responses during the early stages of infection in susceptible and resistant mice. Exp Parasitol **2007**; 115:301–4.
36. Vigario AM, Gorgette O, Dujardin HC, et al. Regulatory $CD4^+CD25^+$ $Foxp3^+$ T cells expand during experimental *Plasmodium* infection but do not prevent cerebral malaria. Int J Parasitol **2007**; 37:963–73.
37. Nie CQ, Bernard NJ, Schofield L, Hansen DS. CD4+ CD25+ regulatory T cells suppress CD4+ T-cell function and inhibit the development of *Plasmodium berghei*-specific TH1 responses involved in cerebral malaria pathogenesis. Infect Immun **2007**; 75:2275–82.
38. Good MF. Identification of early cellular immune factors regulating growth of malaria parasites in humans. Immunity **2005**; 23:241–2.
39. Walther M, Tongren JE, Andrews L, et al. Upregulation of TGF-beta, FOXP3, and CD4+CD25+ regulatory T cells correlates with more rapid parasite growth in human malaria infection. Immunity **2005**; 23:287–96.
40. Pasare C, Medzhitov R. Toll pathway-dependent blockade of CD4+CD25+ T cell-mediated suppression by dendritic cells. Science **2003**; 299:1033–6.
41. Neville LF, Mathiak G, Bagasra O. The immunobiology of interferon-gamma inducible protein 10 kD (IP-10): a novel, pleiotropic member of the C-X-C chemokine superfamily. Cytokine Growth Factor Rev **1997**; 8:207–19.
42. Taylor-Robinson AW. Immunoregulation of malarial infection: balancing the vices and virtues. Int J Parasitol **1998**; 28:135–48.
43. Couper KN, Blount DG, de Souza JB, Suffia I, Belkaid Y, Riley EM. Incomplete depletion and rapid regeneration of Foxp3+ regulatory T cells following anti-CD25 treatment in malaria-infected mice. J Immunol **2007**; 178:4136–46.